analytical chemistry

Letter

Cite This: *Anal. Chem.* XXXX, XXX, XXX−XXX

pubs.acs.org/ac

Detection and Identification of Plant Pathogens on Maize Kernels with a Hand-Held Raman Spectrometer

Charles Farber[†] and Dmitry Kurouski*[,†,‡]

[†]Department of Biochemistry and Biophysics, Texas A&M University, College Station, Texas 77843, United States

[‡]The Institute for Quantum Science and Engineering, Texas A&M University, TAMU 4242, College Station, Texas, 77843, United States

Supporting Information

ABSTRACT: Rapid detection and identification of crop pathogens is essential for improving crop yield. Typical pathogen assaying methods, such as polymerase chain reaction (PCR) or enzyme-linked immunosorbent assay (ELISA), are time-consuming and destructive to the sample. Raman spectroscopy (RS) is a noninvasive nondestructive analytical technique that provides insight on the chemical structure of the specimen. In this study, we demonstrate that using a hand-held Raman spectrometer, in combination with chemometric analyses, we can distinguish between healthy and diseased maize (*Zea mays*) kernels, as well as between different diseases with 100% accuracy. Our analysis is portable and sample-agnostic, suggesting that it could be retooled for other crops and conducted autonomously.

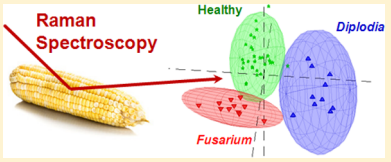

The continuous growth of the human population makes global food security one of the most important aspects of maintaining our civilization. Currently, over a billion people suffer from different kinds of malnutrition due to a lack of sufficient food. There are several strategies to address this issue, one of which is increasing agricultural land areas. Not only is this approach highly destructive to nature, but it is also highly inefficient, as we will need 70% more food by 2050.[1] The second strategy addresses disease-induced damage to crops during growth, harvest, and postharvest processing. Plant diseases make a tremendous impact on crop productivity, causing up to 50% of crop loss.[2] Timely disease diagnosis will reduce costs of pathogen treatment and increase crop yield.

Over the past decade, several imaging and molecular techniques have been developed for disease diagnostics.[3−5] Plant imaging techniques, such as hyperspectral imaging and thermography, are based on detecting changes in the electromagnetic spectrum or in the surface temperature of the plant that are caused by pathogens.[6] These techniques can be conducted remotely with airplanes or unmanned aerial vehicles (UAVs) and therefore are used for monitoring large fields. However, neither hyperspectral imaging nor thermography have disease specificity. At the same time, both are highly sensitive to changes in environmental conditions during measurement, which significantly reduces their accuracy.

Molecular techniques, in contrast, exhibit high pathogen specificity. However, all currently available molecular methods for plant pathogen diagnostics have their own limitations. Specifically, polymerase chain reaction (PCR) is highly sensitive to the quality of reagents, requires initial design of DNA primers for amplification and has limited portability.[7] Immunofluorescence, fluorescent in situ hybridization (FISH) and enzyme-linked immunosorbent assay (ELISA) suffer from photobleaching and are not sensitive to all pathogens.[8,9] Their practical utilization in the field for pathogen analysis is time-consuming and usually very challenging. Flow cytometry provides a wealth of information, but much of this information is not relevant for disease detection.[8] Gas and liquid chromatography (GC and LC) alone or in combination with mass spectrometry (GC- and LC-MS) is very complex, requires time-consuming sample preparation, and has limited portability.[4] These limitations recently catalyzed a push toward developing minimally invasive and substrate general techniques that can be used in the field for confirmatory detection and identification of plant pathogens.

Raman spectroscopy (RS) is a label-free, noninvasive, and nondestructive spectroscopic technique that provides information about the chemical structure of analyzed specimens. Its practical applications span from food chemistry[10] and electrochemistry[11] to forensics[12,13] and materials science.[14] For instance, it has been recently demonstrated that RS can be used to monitor changes in protein secondary structure,[15] conduct forensic analysis of body fluids[12] and detect gun-shot residues.[16] Over the past decade, several companies have developed portable Raman spectrometers, which has enabled utilization of RS directly in the field for applications such as forensics[17] and minerology.[18,19]

Maize, or corn (*Zea mays*), is one the most widely cultivated grains in the world.[20] Its commercial impact is more than 50 billion U.S. dollars alone.[21] Maize is used as livestock feed, raw material in industry, biofuel and as human food. In the current study, we demonstrate that RS can be used for the confirmatory detection and identification of plant pathogens on intact maize kernels. We collected Raman spectra from individual maize

Received: January 15, 2018
Accepted: February 20, 2018
Published: February 20, 2018

ACS Publications © XXXX American Chemical Society

DOI: 10.1021/acs.analchem.8b00222
Anal. Chem. XXXX, XXX, XXX−XXX

kernels using a hand-held portable Rigaku Progeny ResQ spectrometer (Rigaku Analytical Devices, Inc. Wilmington, MA), equipped with a 1064 nm Nd:YAG laser. Experimental details of the Raman measurements can be found in Figure S1. Averaged spectra of healthy maize, as well as maize infected by the fungal pathogens *Aspergillus flavus*, *A. niger*, *Fusarium* spp., or *Diplodia* spp. are shown in Figure 1.

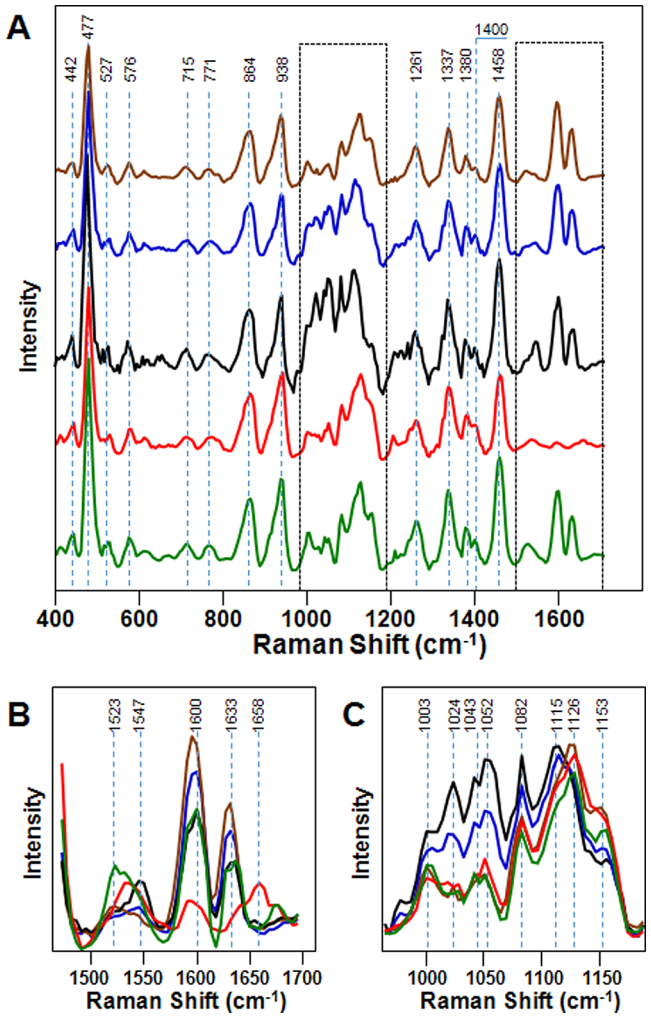

Figure 1. Raman spectra of healthy maize kernels (green) and maize kernels infected by *Aspergillus niger* (brown), *A. flavus* (blue), *Diplodia* spp. (black), and *Fusarium* spp. (red). Spectral acquisition time is 80 s, power 200 mW. For each reported spectrum, 8–15 individual spectra collected from different kernels were averaged. Due to a lack of an internal standard, which can be used for spectral normalization, the reported spectra normalized by 477 cm^{-1} peak height for better visualization. The spectra were baseline corrected by Rigaku Progeny software. GRAMS/AI 7.0 (Thermo Galactic, Salem, NH) was used for spectral processing. Spectra shown are raw baseline corrected, without smoothing.

Typical Raman spectra of healthy kernels exhibit vibrational bands originating from lignin, carbohydrates, proteins, and carotenoids (Figure 1 and Table 1). Lignin shows two vibrational peaks centered at 1600 and 1633 cm^{-1}. The 1600 cm^{-1} peak can be assigned to C–C ring stretching and symmetric C–H vibration.[22] The 1633 cm^{-1} band originates from C═C aromatic ring vibration.[23] We found that these bands nearly disappear in the spectra of *Fusarium*-infected maize. This indicates significant degradation of lignin, associated with *Fusarium* propagation and development in maize kernels. We have also observed a change in the intensity of lignin peaks in the spectra of *A. flavus* and *A. niger*, whereas their intensity did not change much in the spectrum of *Diplodia* (Figure S2). Our findings suggest that these spectral changes are associated with the presence of pathogens in maize kernels.

Table 1. Vibrational Bands and Their Assignments for Healthy and Diseased Maize Kernels

band	vibrational mode	assignment
1658	C═O stretching (amide I)	proteins[24]
1633	C═C–C (ring)	lignin[23]
1600	ν(C–C) aromatic ring + σ(CH)	lignin[22,23]
1547	–C═C– (in plane)	carotenoids[25]
1523	–C═C– (in plane)	carotenoids[25]
1458	δ(CH) + $\delta(CH_2)$ + δ(C–O–H) CH, CH_2, and COH deformations	carbohydrates[10]
1400	δ(C–C–H)	carbohydrates[10]
1380	δ(C–O–H), coupling of the CCH and COH deformation modes	carbohydrates[10]
1337	ν(C–O); δ(C–O–H)	carbohydrates[10]
1261	δ(C–C–H) + δ(O–C–H) + δ(C–O–H)	carbohydrates[10,26]
1153	ν(C–O–C), ν(C–C) in glycosidic linkage, asymmetric ring breathing	carbohydrates[27]
1126	ν (C–O) + ν(C–C) + δ(C–O–H)	carbohydrates[10]
1115	C–OH bending	carbohydrates[28]
1082	ν(C–O) + ν(C–C) + δ(C–O–H)	carbohydrates[10]
1052	ν(C–O) + ν(C–C) + δ(C–O–H)	carbohydrates[10]
1043	δ(C–OH)	carbohydrates[28,29]
1024	δ(C–OH)	carbohydrates[28,29]
1003	ν_3 (C–CH_3 stretching) and phenylalanine	carotenoids[24,30]
938	δ(C–O–C) + δ(C–O–H) + ν(C–O) α-1,4 glycosidic linkages	carbohydrates[10]
864	δ(C–C–H) + δ(C–O–C) glycosidic bond; anomeric region	carbohydrates[10]
771	δ(C–C–O)	carbohydrates[10]
715	δ(C–C–O) related to glycosidic ring skeletal deformations	carbohydrates[10]
576	δ(C–C–O) + τ(C–O)	carbohydrates[10]
527	S–S *gauche–gauche–trans*	protein[31]
477	CCO and CCC deformations; Related to glycosidic ring skeletal deformations δ(C–C–C) + τ(C–O) scissoring of C–C–C and out-of-plane bending of C–O	carbohydrates[10]
442	skeletal modes of pyranose ring	carbohydrates[10]

A typical Raman spectrum of a protein exhibits a carbonyl vibration of the peptide bond at 1640–1670 cm^{-1}, known as the amide I band.[24] We observed a distinct peak around 1658 cm^{-1} in the spectra of *Fusarium*-infected maize kernels, indicating that growth of this pathogen is strongly associated with the deposition of protein in the maize kernels.

Vibrational bands around 1530 cm^{-1} originate from –C═C– in-plane vibrations and can be assigned to carotenoids (Figure 1B).[25] Longer chain polyenes in these molecules show blue-shifted vibrational bands, whereas those with shorter chains have red-shifted bands.

In all spectra of maize kernels, we observed two vibrational bands centered at 1523 and 1547 cm^{-1}. In the spectrum of healthy maize kernels, carotenoids showed an intense peak at 1523 cm^{-1}. In contrast, in all pathogen-infected maize kernels except *A. niger*, the peak at 1547 cm^{-1} was more intense than the peak at 1523 cm^{-1}. This suggests that growth of these pathogens on maize kernels could be associated with degradation and fragmentation of host carotenoids. Alter-

DOI: 10.1021/acs.analchem.8b00222
Anal. Chem. XXXX, XXX, XXX–XXX

Table 2. Accuracy of Classification by OPLS-DA for Each Class of Maize Kernel

	members	correct	*A. niger*	*A. flavus*	*Diplodia*	*Fusarium*	healthy	no class (YPred ≤ 0)
A. niger	10	100%	10	0	0	0	0	0
A. flavus	17	100%	0	17	0	0	0	0
Diplodia	10	100%	0	0	10	0	0	0
Fusarium	11	100%	0	0	0	11	0	0
healthy	29	100%	0	0	0	0	29	0
no class	0		0	0	0	0	0	0
total	77	100%	10	17	10	11	29	0
Fisher's prob.	2.5e-033							

natively, it is possible that these pathogens produce specific short-chain carotenoids. Finally, observed spectral changes of carotenoids in maize kernels could be attributed to their conversion to apocarotenoids, signaling molecules that are synthesized by plants as a stress response.[32] Further studies are required to elucidate the actual cause of the change in carotenoids peaks in healthy and pathogen-infected corn. In addition to the observed frequency shift, we also observed an intensity reduction at the 1523 cm^{-1} peak in in all infected kernels, providing further support for our hypothesis that host carotenoids are affected by fungal infection. Therefore, one may expect that the 1547 cm^{-1} band can be used as a marker of the maize kernel healthiness. It was interesting to find that in the Raman spectrum of *A. niger*, the two carotenoids peaks had much more similar intensity ratio to a spectrum of healthy kernel than in the spectra of diseased kernels. This suggests that *A. niger* and *A. flavus* may have different metabolic strategies and consequently cause dissimilar changes to maize carotenoids. Electromagnetic excitation within 400−600 nm spectral region can be used to do resonance Raman studies of maize carotenoids.[30] This will lead to a million-fold increase in their signals allowing for better understanding of the structural changes in the carotenoid component of maize associated with fungal infections.

Carbohydrates, including monomeric sugars and starch, are the major components of maize kernels.[20] Therefore, most of the observed vibrational bands originate from these molecules.[10] Vibrational bands at 1153, 938, and 864 cm^{-1} are associated with C−O−C vibration, which is typical for starch. Raman bands at 1115, 1082, 1052, 1043, and 1024 cm^{-1} represent C−O−H vibrations (Figure 1C). Hydrolysis of starch will result in an increase in monomeric sugars and, consequently, the increase in intensities of C−O−H vibrations. We observed such a change in C−O−C and C−O−H vibrations in the spectra of *Diplodia* and *A. flavus* (Figures 1C and S2). This indicates that pathogenic activity of these fungi in maize kernels is associated with breakdown of maize starch to monomeric sugars. We observed the opposite trend in the *A. niger* and *Fusarium*-infected kernels. Specifically, the intensity of C−O−C band increased in the spectra of *A. niger* and *Fusarium* comparing to the spectrum of healthy maize (Figures 1C and S2). This observation suggests that *A. niger* and *Fusarium* are associated with conversion of maize monomeric sugars into their polymeric hydrocarbons.

It is important to ask whether the proposed spectroscopic approach allows for the detection of actual pathogens or the observed spectral changes report only pathogen-related structural changes of the maize kernel. A detailed spectral analysis, which was discussed above, does not let us disentangle these two possibilities. Work to address this question by the spectroscopic analysis of all chemical components of those plant pathogens, such as their metabolites and toxins, is under way in our laboratory.

Next, we used multivariate data analysis[33] to determine whether RS can be used for the quantitative detection and identification of plant pathogens. All collected Raman spectra were imported into SIMCA 14 (Umetrics, Umeå, Sweden) for statistical analysis and scaled to unit variance to give all spectral regions equal importance. Orthogonal partial least-squares discriminant analysis (OPLS-DA) was performed to determine the number of predicting and orthogonal significant components and identify spectral regions that best explain the separation between the classes.[34] Unlike the ordinary partial least-squares discriminant analysis (PLS-DA), OPLS-DA separates the systematic variation in spectral data into two parts, one part (predictive) that explains the separation among classes and the other (orthogonal) that does not account for the separation of classes. In this iteration of OPLS-DA, the wavenumbers with the variable importance (VIP) of less than 1.0 were excluded to reduce the noise and improve the predictive power of the model.[30] The final model, containing 4 predictive components, 3 orthogonal components, and 391 out of 512 original wavenumbers, was used to generate the misclassification table (Table 2) and the loadings plot (Figure 2).

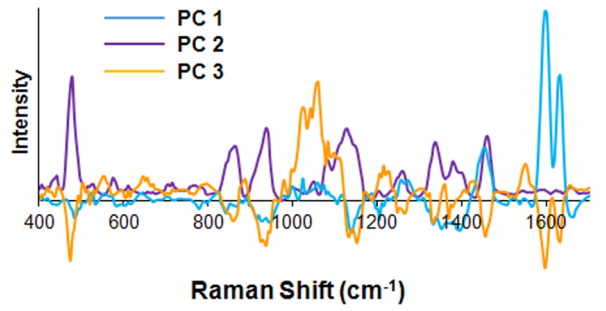

Figure 2. Loading plot of the three predictive components (PC) in the Raman spectra of maize kernels.

The first three predictive components (PC; Figure 2) explain 23%, 19%, and 18% of the variation between classes, respectively, which collectively accounts for 60% of the total class-to-class variation. Absolute intensities in the loadings spectra are proportional to the percentage of the total variation between classes explained by each wavenumber within each component. The model identified the carbohydrates peak at 477 cm^{-1} (PC1), lignin peaks at 1600 and 1633 cm^{-1} (PC2), the carotenoid band at 1547 cm^{-1} (PC3), the peptide bond vibration at 1658 cm^{-1} (PC2) and the 1000−1160 cm^{-1} region (PC1 and PC3) as the strongest predictors of the maize pathogens, which supports the conclusions of our qualitative

DOI: 10.1021/acs.analchem.8b00222
Anal. Chem. XXXX, XXX, XXX−XXX

spectral analysis above. The model explained 97% of the variation (R2X) in the spectra and 69% (R2Y) of the variation between the classes. Furthermore, the model correctly assigned all 77 spectra to their classes (Table 2). This indicates that coupling of OPLS-DA with RS allows for a 100% accurate detection and identification of these four pathogens on maize kernels.

Our results clearly demonstrate that RS can be used for confirmatory, noninvasive and nondestructive detection and identification of plant pathogens directly on maize kernels. We demonstrated that the combination of chemometric analysis and RS enables us to distinguish between healthy and infected kernels with 100% accuracy. Our results suggest that the proposed spectroscopic approach can be used for pathogen detection and identification on other crops, such as sorghum, rice and wheat. This is extremely important to prevent widespread pathogen propagation. Pathogen-infected crops also contain highly toxic and carcinogenic compounds, such as aflatoxin[35] and fumonisin.[36] Thus, the proposed spectroscopic detection and identification of plant pathogens in intact grain will help to reduce consumption of infected grain and minimize aflatoxin- and fumonisin-induced cancer in numerous developing counties.

■ ASSOCIATED CONTENT

Supporting Information

The Supporting Information is available free of charge on the ACS Publications website at DOI: 10.1021/acs.analchem.8b00222.

Detailed description of spectra acquisition methods and accompanying experimental setup are shown in Figure S1. Relative intensity chart and corresponding table of peak intensities at the given wavenumbers are shown in Figure S2 (PDF).

■ AUTHOR INFORMATION

Corresponding Author

*E-mail: dkurouski@tamu.edu. Tel.: 979-458-3448.

ORCID

Dmitry Kurouski: 0000-0002-6040-4213

Notes

The authors declare no competing financial interest.

■ ACKNOWLEDGMENTS

We are grateful to AgriLife Research of Texas A&M for the provided financial support. We also acknowledge Governor's University Research Initiative (GURI) grant program of Texas A&M University, GURI Grant Agreement No. 12-2016, and the Texas A&M University System Chancellor's Research Initiative. We are grateful to Dr. Michael Kolomiets and John Bennett from the Department of Plant Pathology and Microbiology for the provided maize samples.

■ REFERENCES

(1) Food and Agriculture Organization of the United Nations, How to Feed the World 2050; http://www.fao.org/fileadmin/templates/wsfs/docs/Issues_papers/HLEF2050_Global_Agriculture.pdf, 2009.

(2) Savary, S.; Ficke, A.; Aubertot, J.-N.; Hollier, C. *Food. Secur.* **2012**, *4*, 519−537.

(3) Fang, Y.; Ramasamy, R. P. *Biosensors* **2015**, *5*, 537−561.

(4) Martinelli, F.; Scalenghe, R.; Davino, S.; Panno, S.; Scuderi, G.; Ruisi, P.; Villa, P.; Stroppiana, D.; Boschetti, M.; Goulart, L. R.; Davis, C. E.; Dandekar, A. M. *Agron. Sustainable Dev.* **2015**, *35*, 1−25.

(5) Yeturu, S.; Vargas Jentzsch, P.; Ciobotă, V.; Guerrero, R.; Garrido, P.; Ramos, L. A. *Anal. Methods* **2016**, *8*, 3450−3457.

(6) Mahlein, A.-K.; Oerke, E.-C.; Steiner, U.; Dehne, H.-W. *Eur. J. Plant Pathol.* **2012**, *133*, 197−209.

(7) Schaad, N. W.; Frederick, R. D. *Can. J. Plant Pathol.* **2002**, *24*, 250−258.

(8) Chitarra, L. G.; Bulk, R. W. v. d. *Eur. J. Plant Pathol.* **2003**, *109*, 407−417.

(9) Wallner, G.; Amann, R.; Beisker, W. *Cytometry* **1993**, *14*, 136−143.

(10) Almeida, M. R.; Alves, R. S.; Nascimbem, L. B.; Stephani, R.; Poppi, R. J.; de Oliveira, L. F. *Anal. Bioanal. Chem.* **2010**, *397*, 2693−2701.

(11) Zeng, Z. C.; Hu, S.; Huang, S. C.; Zhang, Y. J.; Zhao, W. X.; Li, J. F.; Jiang, C.; Ren, B. *Anal. Chem.* **2016**, *88*, 9381−9385.

(12) Kelly, V.; Lednev, I. K. *Anal. Chem.* **2009**, *81*, 7773−7777.

(13) López-López, M.; Delgado, J. J.; García-Ruiz, C. *Forensic Sci. Int.* **2013**, *231*, 1−5.

(14) Cantarero, A. *Procedia Mater. Sci.* **2015**, *9*, 113−122.

(15) Kurouski, D.; Washington, J.; Ozbil, M.; Prabhakar, R.; Shekhtman, A.; Lednev, I. K. *PLoS One* **2012**, *7*, e36989.

(16) Bueno, J.; Lednev, I. K. *Anal. Methods* **2013**, *5*, 6292−6296.

(17) Kurouski, D.; Van Duyne, R. P. *Anal. Chem.* **2015**, *87*, 2901−2906.

(18) Jehlička, J.; Culka, A.; Baštová, M.; Bašta, P.; Kuntoš, J. *Philos. Trans. R. Soc., A* **2016**, *374*, 0042.

(19) Košek, F.; Culka, A.; Jehlička, J. *J. Raman Spectrosc.* **2017**, *48*, 1494−1502.

(20) National Corn Growers Association, World of Corn 2017; http://www.worldofcorn.com/pdf/_WOC_2017.pdf, 2017.

(21) International Grain Council, Grain Market Report; https://www.igc.int/downloads/gmrsummary/gmrsumme.pdf, 2017.

(22) Kang, L.; Wang, K.; Li, X.; Zou, B. *J. Phys. Chem. C* **2016**, *120*, 14758−14766.

(23) Pompeu, D. R.; Larondelle, Y.; Rogez, H.; Abbas, O.; Pierna, J. A. F.; Baeten, V. *Biotechnol. Agron. Soc. Environ.* **2017**, *22*, 1−16.

(24) Kurouski, D.; Van Duyne, R. P.; Lednev, I. K. *Analyst* **2015**, *140*, 4967−4980.

(25) Adar, F. *Spectroscopy* **2017**, *32*, 12−20.

(26) Cael, J. J.; Koenig, J. L.; Blackwell, J. *Biopolymers* **1975**, *14*, 1885−1903.

(27) Wiercigroch, E.; Szafraniec, E.; Czamara, K.; Pacia, M. Z.; Majzner, K.; Kochan, K.; Kaczor, A.; Baranska, M.; Malek, K. *Spectrochim. Acta, Part A* **2017**, *185*, 317−335.

(28) Edwards, H. G. M.; Farwell, D. W.; Webster, D. *Spectrochim. Acta, Part A* **1997**, *53*, 2383−2392.

(29) Walton, A. *Biopolymers*; Academic Press: New York, 1973.

(30) Tschirner, N.; Brose, K.; Schenderlein, M.; Zouni, A.; Schlodder, E.; Mroginski, M. A.; Hildebrandt, P.; Thomsen, C. *Phys. Status Solidi B* **2009**, *246*, 2790−2793.

(31) Rygula, A.; Majzner, K.; Marzec, K. M.; Kaczor, A.; Pilarczyk, M.; Baranska, M. *J. Raman Spectrosc.* **2013**, *44*, 1061−1076.

(32) Altangerel, N.; Ariunbold, G. O.; Gorman, C.; Alkahtani, M. H.; Borrego, E. J.; Bohlmeyer, D.; Hemmer, P.; Kolomiets, M. V.; Yuan, J. S.; Scully, M. O. *Proc. Natl. Acad. Sci. U. S. A.* **2017**, *114*, 3393−3396.

(33) Shashilov, V. A.; Lednev, I. K. *Chem. Rev.* **2010**, *110*, 5692−5713.

(34) Eriksson, L.; Byrne, T.; Johansson, E.; Trygg, J.; Vikstrom, C. *Multi- and Megavariate Data Analysis Basic Principles and Applications*, 3rd revised ed.; Umetrics Academy, 2013.

(35) Williams, J. H.; Phillips, T. D.; Jolly, P. E.; Stiles, J. K.; Jolly, C. M.; Aggarwal, D. *Am. J. Clin. Nutr.* **2004**, *80*, 1106−1122.

(36) Norred, W. P.; Voss, K. A. *J. Food Prot.* **1994**, *57*, 522−527.

DOI: 10.1021/acs.analchem.8b00222
Anal. Chem. XXXX, XXX, XXX−XXX